Blast Preconditioning Protects Retinal Ganglion Cells and Reveals Targets for Prevention of Neurodegeneration Following Blast-Mediated Traumatic Brian Injury

Matthew M. Harper,[1,2] Addison W. Woll,[1,2] Lucy P. Evans,[3,4] Michael Delcau,[1,2] Abhigna Akurathi,[1] Adam Hedberg-Buenz,[1,5] Dana A. Soukup,[5] Nickolas Boehme,[1,2] Marco M. Hefti,[6] Laura M. Dutca,[1,2] Michael G. Anderson,[1,2,5] and Alexander G. Bassuk[4,7]

[1]The Iowa City Department of Veterans Affairs Medical Center, Center for the Prevention and Treatment of Visual Loss, Iowa City, Iowa
[2]Department of Ophthalmology and Visual Sciences, University of Iowa, Iowa City, Iowa, United States
[3]Medical Scientist Training Program, University of Iowa, Iowa City, Iowa, United States
[4]Department of Pediatrics, University of Iowa, Iowa City, Iowa, United States
[5]Department of Molecular Physiology and Biophysics, University of Iowa, Iowa City, Iowa, United States
[6]Department of Pathology, University of Iowa, Iowa City, Iowa, United States
[7]Department of Neurology, University of Iowa, Iowa City, Iowa, United States

Correspondence: Matthew M. Harper, Center for the Prevention and Treatment of Visual Loss, Department of Veterans Affairs, The University of Iowa, Department of Ophthalmology and Visual Sciences, 601 Highway 6 West, Iowa City, IA 52772, USA; matthew-harper@uiowa.edu.

Submitted: May 20, 2019
Accepted: August 22, 2019

Citation: Harper MM, Woll AW, Evans LP, et al. Blast preconditioning protects retinal ganglion cells and reveals targets for prevention of neurodegeneration following blast-mediated traumatic brain injury. *Invest Ophthalmol Vis Sci*. 2019;60:4159–4170. https://doi.org/10.1167/iovs.19-27565

Purpose. The purpose of this study was to examine the effect of multiple blast exposures and blast preconditioning on the structure and function of retinal ganglion cells (RGCs), to identify molecular pathways that contribute to RGC loss, and to evaluate the role of kynurenine-3-monooxygenase (KMO) inhibition on RGC structure and function.

Methods. Mice were subjected to sham blast injury, one single blast injury, or three blast injuries separated by either 1 hour or 1 week, using a blast intensity of 20 PSI. To examine the effect of blast preconditioning, mice were subjected to sham blast injury, one single 20-PSI injury, or three blast injuries separated by 1 week (5 PSI, 5 PSI, 20 PSI and 5 PSI, 5 PSI, 5 PSI). RGC structure was analyzed by optical coherence tomography (OCT) and function was analyzed by the pattern electroretinogram (PERG). BRN3A-positive cells were quantified to determine RGC density. RNA-seq analysis was used to identify transcriptional changes between groups.

Results. Analysis of mice with multiple blast exposures of 20 PSI revealed no significant differences compared to one 20-pounds per square inch (PSI) exposure using OCT, PERG, or BRN3A cell counts. Analysis of mice exposed to two preconditioning 5-PSI blasts prior to one 20-PSI blast showed preservation of RGC structure and function. RNA-seq analysis of the retina identified multiple transcriptomic changes between conditions. Pharmacologic inhibition of KMO preserved RGC responses compared to vehicle-treated mice.

Conclusions. Preconditioning protects RGC from blast injury. Protective effects appear to involve changes in KMO activity, whose inhibition is also protective.

Keywords: blast TBI, brain injury, neuroprotection, retinal ganglion cell, kyneurinine-3-monooxygenase

Blast-mediated traumatic brain injury (bTBI) is caused by exposure to blast waves in military combat or by explosions that affect civilians. Blast waves travel at supersonic speeds[1] and interact with tissues to create acute damage to neural tissues, as well as activating mechanisms that lead to chronic neuronal damage and dysfunction. Multiple studies have demonstrated significant central nervous system (CNS) damage after blast exposure in both humans and laboratory models.[2–14] Residual effects of blast exposure in patients include decreased auditory function,[13,15–17] increased incidence of posttraumatic headache,[18] development of PTSD,[19] difficulty with cognitive tasks,[20] and an increased incidence of affective disorders.[21] Damage to and dysfunction of the visual system are common after bTBI, which results in anatomic damage, convergence difficulties, decreased visual acuity, light sensitivity, ocular motility, and increased visual field loss.[10,22]

Blast waves are created by an explosion and radiate outward from the source.[23] The intensity of the blast wave decays exponentially as the distance from the blast center increases. Many patients experiencing low-intensity blasts may not present with overt physical trauma, and may not have these exposures documented. There is evidence that blast exposure can result in cumulative damage to the CNS,[24–26] which may explain some of the variability in outcomes between individuals exposed to similar high-intensity blasts.[27] Repetitive blast exposure can affect multiple aspects of the CNS. A multi-symptom survey showed that individuals with repeated blast exposure had significantly more symptoms (including cognitive, affective, and somatic), a greater number of interfering

symptoms, and a greater number of severe symptoms compared to the non–blast-exposed cohort.[28] A significant amount of research has focused on cognitive outcomes following blast injury due to the potential effect on quality of life. A study of veterans exposed to repeated blast injury demonstrated decreased verbal fluency, cognitive processing, attention, and working memory, which correlated with a decreased cerebral metabolic rate.[25] Further neuroimaging techniques have shown that decreased performance on neurocognitive tests due to repetitive blast exposures correlated with decreased task performance measured using functional magnetic resonance imaging.[29] Multiple biomarkers have been proposed to detect individuals with multiple blast-related symptoms, such as decreased performance on a stepping-in-place task in active service members,[30] and serum biomarkers. One study of serum biomarkers from individuals with repeated blast exposure showed that individuals with high levels of ubiquitin C-terminal hydrolase-L1, αII-spectrin breakdown product, and glial fibrillary acidic protein had lower neurocognitive performance compared to individuals expressing low levels of these biomarkers.[31]

The first studies examining the effects of repetitive blast-mediated TBI on the visual system have shown that these injuries can be cumulative, which has also been observed in a weight-drop model.[32–34] Aside from the effect of multiple TBIs on the visual system, the effect of repetitive TBIs on the brain has been extensively studied using various models of open-head and closed-head injury (for review see Ref. 35), which induce a range of severities from mild to severe.[35] Multiple TBIs have been shown to exacerbate mitochondrial and metabolic dysregulation,[36] increase neuronal death,[37] increase the astrocytic response,[38–40] increase microglial activation,[38,41] and exacerbate axonal damage[37–39,41–46] compared to single injuries. The effect of multiple TBIs extends beyond molecular events into behavioral phenotypes. Repeated TBIs have been shown to result in behavioral/cognitive impairment in the acute to subacute time points after injury,[41,47] although one study reports sustained motor and memory deficits after injury.[48] The timing of the secondary injury relative to the first seems to have an effect on these outcomes. Multiple TBIs with short inter-TBI intervals have been shown to result in permanent cognitive deficits,[42,49,50] while increased inter-TBI intervals may result in a preconditioning effect that has been shown to be protective.[36,50]

The effect of repetitive blast exposures on the brain has been less well characterized than for non–blast-mediated TBIs. Multiple blast exposures in preclinical models lead to increased blood–brain barrier permeability[51] as well as seizures,[52] in addition to axonal damage and white matter injury,[32,53,54] compared to one single blast exposure. Laboratory models have shown decreased metabolic rate,[55] which may lead to increased oxidative stress.[56] Mitochondrial dysfunction after repeated blast exposure has been observed,[57] which may be a response to injury or an initiating event in neuronal dysfunction. Repetitive blast exposure with a 24-hour inter-blast interval showed increased microglial staining, but no apparent changes in cell death, damaged axons, or damaged dendrites compared to animals receiving a single blast injury.[58] There was, however, decreased hippocampal long-term potentiation in animals with multiple blast injuries compared to single blast injuries.[58] Taken together, these studies suggest that repetitive blast injuries may lead to increased neuronal dysfunction compared to single blast injuries, although the interblast interval and blast intensity should be taken into account when making direct comparisons.

It has been observed that single blast exposure results in activation of molecular pathways and networks that lead to death and dysfunction of affected neurons, either directly or through development of chronic diseases including chronic traumatic encephalopathy or Alzheimer's disease.[2,59–61] These mechanisms are varied and can include an increase in phosphorylated tau protein and beta amyloid deposition, inflammation, oxidative stress, mitochondrial dysfunction, and activation of microglia.[62] The activation of these pathways can lead to cell death in experimental models through various molecular mechanisms that depend on the blast intensity and resultant tissue loading.[63–65] The response to blast exposure may also depend on the physical properties of the tissue[66–69] and physical properties surrounding the tissue, such as the shape of the face and the use of eye armor in the case of ocular injury.[70] It is likely that many of these pathways are downstream of initiating molecular events causing neuronal death and dysfunction, particularly in bTBI that does not result in overt necrosis or vascular damage. Defining these initiating mechanisms is an important step toward development of neuroprotective or rehabilitative strategies to treat the symptoms of bTBI.

The purpose of this study was to investigate the effects of multiple blast waves on the structure and function of retinal ganglion cells (RGCs) for interblast intervals of 1 hour or 1 week. We also sought to determine if preconditioning with low-level blast exposures modulates the effect of subsequent higher-intensity blast exposures. We used RNA-seq analysis of blast-injured retinas to define specific molecules involved in neuronal death and dysfunction following blast exposure. One molecule that was identified through analysis of RNA-seq was kynureinine-3-monooxygenase (KMO). We also sought to test the functional role of KMO by inhibiting it with Ro-61-8048 in mice exposed to blast injury.

Methods

Animals

All animal studies were conducted in accordance with the ARVO Statement for the Use of Animals in Ophthalmic and Vision Research and were approved by the Iowa City Department of Veterans Affairs Institutional Animal Care and Use Committee. Male C57BL6/J mice were purchased from The Jackson Laboratory (Bar Harbor, ME, USA) and subjected to blast injury at 8 weeks of age. A total of 144 mice were used for the purpose of this study.

Blast Injury Induction

An enclosed blast chamber was used for the purpose of these studies, one-half of which was pressurized, with a 13-cm-diameter opening between the chamber halves, as described previously.[71,72] A Mylar membrane (Mylar A, 0.00142 gauge; Country Plastics, Ames, IA, USA) was placed over the opening on the pressurized side of the chamber. The unpressurized side of the tank contained a padded polyvinyl chloride (PVC) protective restraint for positioning of an anesthetized mouse (see Mohan et al.,[72] for diagram). To create the blast wave, air was pumped into the pressurized side of the tank to 20 or 5 pounds per square inch (PSI) to rupture a membrane. Using this model, a blast wave is produced with the following characteristics after rupture of 20-PSI membranes: 140.92 ± 10.82-kPa peak pressure with a 7.0 ± 2.09-ms positive phase duration (mean ± SD). Rupture of 5-PSI membranes generated a blast wave of 39.64 ± 11.7-kPa peak pressure, with a 3 ± 1.41-ms positive phase duration (mean ± SD). The pressure was measured using a sensor 1 cm in diameter placed directly below the head of the mouse. Prior to blast wave induction, mice were anesthetized with a combination of ketamine (0.03

mg/g body weight, intraperitoneal, IP) and xylazine (0.005 mg/g body weight, IP) and positioned within the unpressurized half of the blast chamber with the left side of the head oriented toward the source of the blast wave. Only the head of the mouse was exposed to the blast wave, with the rest of the body shielded. The head of the mouse was unrestrained during blast wave exposure, but was prevented from coming into contact with any hard surface by thick foam placed directly behind the head. Non–blast-exposed mice were anesthetized and placed in the blast chamber, but did not receive a blast exposure (referred to as sham blast). After blast or sham blast exposure, mice were placed on a heating pad to facilitate recovery from general anesthesia and to prevent hypothermia. Xylazine anesthesia was reversed with yohimbine chloride (0.001 mg/g, IP) to facilitate the recovery from anesthesia. Blast TBI and sham groups of mice received analgesic via subcutaneous injection (0.1 mL/20 g body weight) of buprenorphine (0.003 mg/mL) immediately after recovery from the procedure. Mice receiving multiple blast injuries underwent the same procedure, with sham-blasted mice receiving the same dose of anesthetic. Blast exposures were separated by a period of 1 hour or 1 week at 20 PSI. Mice receiving multiple blast injuries were analyzed and tissue was collected 16 weeks following the final blast exposure. Mice utilized to study the effects of preconditioning underwent blast or sham injury 1 week apart, with analysis and tissue collection occurring 8 weeks following the first blast exposure or sham exposure. Sham and blast exposure occurred at the same time for each group, and animals were the same age at the end of each experiment. For blast preconditioning, mice were treated in the following groups: sham, sham, sham; sham, sham, 20 PSI; 5 PSI, 5 PSI, 5 PSI; and 5 PSI, 5 PSI, 20 PSI. Mice utilized for RNA-seq were exposed to two blasts separated by a period of 1 week, with tissue collected 5 days following the last blast exposure. The blast groups analyzed were 5 PSI, 5 PSI; sham, 20 PSI; and 5 PSI, 20 PSI. A summary of blast experimental design is presented in Supplementary Figure S1.

Pattern-Evoked Electroretinography

Pattern-evoked electroretinography (PERG) was used to objectively measure the function of RGCs by recording the amplitude of the PERG waveform following bTBI. Mice were anesthetized with a combination of ketamine (0.03 mg/g, IP), xylazine (0.005 mg/g, IP), and acepromazine (0.002 mg/g, IP) and were placed on a heated animal holder. The eye of each mouse was positioned 10 cm from the stimulus monitor. All recordings were obtained and presented from the eye facing the blast wave. PERG responses were evoked using alternating, reversing, black and white vertical stimuli delivered on a light-emitting diode monitor (Jorvec, Miami, FL, USA). A subdermal recording electrode was placed under the skin on the nose of the animal extending to the snout, equidistant from each eye, as previously described.[73] A reference needle electrode was placed at the base of the head, and a ground electrode was placed at the base of the tail to complete the circuit. Each animal was placed at the same fixed position in front of the monitors to prevent recording variability due to animal placement. Stimuli (18° radius visual angle subtended on full field pattern, 1.5-cm-high × 14-cm-wide bars, 2 reversals per second, 372 averaged signals with cutoff filter frequencies of 1–30 Hz, 98% contrast, 80 cd/m^2 average monitor illumination intensity using luminance-matched pattern reversals to exclude outer retinal contributions) were delivered under mesopic conditions (8.5-lux room luminance) without dark adaptation. A diffuser placed over the pattern on the monitor did not elicit a measurable evoked potential, further ensuring that the electrical responses were elicited from RGCs. The PERG response was evaluated by measuring the amplitude (peak to trough) and implicit time of the waveform, as previously described.[74,75] Data are presented from the left eye, which was directly exposed to blast injury. Mice were examined with a handheld slit-lamp prior to PERG analysis to ensure that no anterior segment damage was present. Analysis of all visual outcomes was obtained only in the left eye to study the effect of primary blast injury.

Spectral-Domain Optical Coherence Tomography

Spectral-domain optical coherence tomography (SD-OCT) analysis was performed using a Spectralis SD-OCT (Heidelberg Engineering, Vista, CA, USA) imaging system coupled with a 25D lens for mouse ocular imaging (Heidelberg Engineering). Mice were anesthetized with a combination of ketamine (0.03 mg/g; IP) and xylazine (0.005 mg/g; IP) and placed on a heating pad to maintain body temperature. Pupils were dilated using a 1% tropicamide solution. The cornea was moisturized with a saline solution. Volume scans (49-line dense array, 15 A-scans per B-scan, 20° scan angle, 20° × 25° scan area) positioned directly over the optic nerve head were performed to quantify the retinal ganglion cell complex (RGCC) thickness (retinal nerve fiber layer + ganglion cell layer + inner plexiform layer), the outer nuclear layer thickness, and the total retinal thickness from the inner limiting membrane to the external limiting membrane. One single B-scan was analyzed by an individual masked to the treatment of the mouse in the superior retina, approximately 150 μm from the peripapillary region. All scans were analyzed by excluding blood vessels from the RGCC thickness calculation.

Immunohistochemical-Based RGC Quantification

After euthanasia of mice, whole eyes were enucleated and the posterior cups dissected and fixed for a total of 4 hours in 4% paraformaldehyde. The immunohistochemical labeling of BRN3A was performed as previously described.[76] Briefly, the posterior cups were incubated in a 0.3% Triton X-100 solution in phosphate-buffered saline (PBST) overnight at 37°C; retinas were dissected and bleached in a 3% hydrogen peroxide solution in 1% sodium phosphate buffer for 3 hours at room temperature. Retinas were permeabilized for 15 minutes at −80°C in PBST, blocked in a 2% normal donkey serum in PBST overnight, and immunohistochemically labeled using an anti-BRN3A antibody (1:200; sc-8429; Santa Cruz Biotechnology, Dallas, TX, USA) in 2% normal donkey serum, 1% Triton X-100, and 1% dimethyl sulfoxide (DMSO) at 4°C for two nights, followed by incubation with a secondary antibody (1:200; Alexa Fluor 488 donkey anti-goat; Invitrogen, Waltham, MA, USA) for 4 hours at room temperature. They were then counterstained with TO-PRO-3 Iodide (1:1000; Molecular Probes, Eugene, OR, USA), transferred to glass microscopy slides and flat-mounted using ProLong Diamond Antifade Mountant (Fisher Scientific, Hampton, NH, USA), and cover-slipped. Flat-mounted retinas were imaged by confocal microscopy (Zeiss LSM 710, White Plains, NY, USA) at a total magnification of ×400. For each retina, 12 confocal images were collected (1024 × 1024 px, 0.18-mm^2 image area) from nonoverlapping fields at each of three zones of eccentricity (four central, four midperipheral, four peripheral), with z-stacks of three to five images collected for each image. Images of BRN3A-labeled nuclei were processed in ImageJ (National Institutes of Health, Bethesda, MD, USA), by first Z-projecting at maximum intensity, followed by the Subtract Background tool with rolling ball radius set to 35 pixels, followed by the Smooth tool. Images were then converted to binary using Huang thresholding. Binary images were further processed

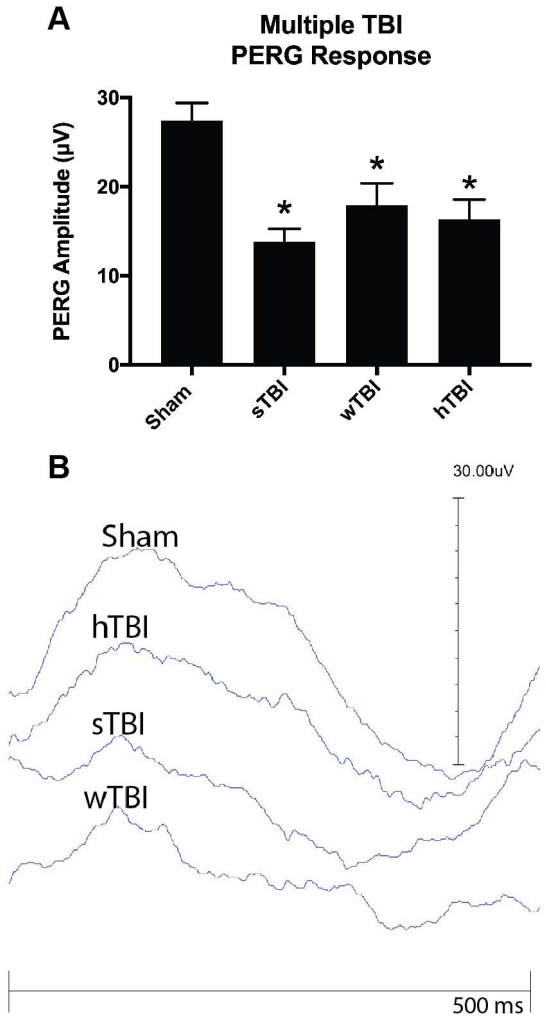

FIGURE 1. Multiple bTBI exposures do not result in greater RGC deficits than one single exposure. PERG analysis of mice exposed to sham blast (sham, $n = 16$), one single blast-mediated TBI (sTBI, $n = 15$), three blast-mediated TBIs separated by 1 week (wTBI, $n = 16$), and three blast-mediated TBIs separated by 1 hour (hTBI, $n = 13$). A decline in the PERG amplitude was observed in mice receiving a single blast exposure ($P = 0.0001$), multiple blast exposures with a 1-week interblast interval ($P = 0.0040$), and multiple blast exposures with a 1-hour interval ($P = 0.0014$, 1-way ANOVA with Dunnett's multiple comparison test). There was no difference when comparing the PERG amplitude of sTBI mice to either the wTBI ($P = 0.3596$) or hTBI ($P = 0.7430$) groups of mice (**A**, **B**).

using the Open, Watershed, and Fill Holes functions. To count BRN3A-positive cells, the Analyze Particles function was applied to the BRN3A images with particle size set to 20 to 150 μm^2 and circularity 0-1. Three retinas required manual counting of the BRN3A-positive RGCs due to faint antibody staining.

Retina Harvest for RNA-seq

Mice were anesthetized using CO_2 and euthanized with cervical dislocation. Only the left eye of each mouse was used for gene expression studies. Immediately following euthanasia, the eye was sprayed with RNAzap (#R2020; Invitrogen, Thermo Fisher Scientific, Waltham, MA, USA). A small incision was made in the eye, permitting the quick removal of the lens. Using RNA-free forceps, the retina was removed by gently squeezing the eyecup from the optic nerve upward, in intervals until the retina was completely dislodged. Retinas were placed in 1:100 β-mercaptoethanol:RLT lysis buffer (#74104, RNeasy Mini Kit; Qiagen, Germantown, MD, USA) and flash frozen in liquid nitrogen. RNA isolation was performed using a modified protocol and a Qiagen RNeasy Mini kit. Samples were analyzed using a NanoDrop 2000 Spectrophotometer (Thermo Fischer Scientific), then flash frozen in liquid nitrogen and stored at –80°C. Due to the strong temporal gene regulation in the retina, samples from each of the three experimental groups were collected in trios not spanning more than 15 minutes.

RNA Sequencing

Samples were delivered to the Genomics Division of the Iowa Institute of Human Genetics, University of Iowa Carver College of Medicine, for library preparation. The quality and quantity of the RNA were determined. The 24 samples were assigned individual barcodes during library preparation and mRNA amplification. All 24 libraries were pooled together, and run over two sequencing lanes on an Illumina (San Diego, CA, USA) HiSeq 4000 Genome Sequencer generating 75 bp-paired end reads. Reads were aligned to the mm10 reference genome using STAR.[77,78] We used featureCounts from the subreads package to quantify transcripts at the gene level.[79] Downstream analyses used the R packages DESeq2[80] to determine differential expression, VariancePartition[81] to identify sources of variance, and ggplot2 for data visualization.[82] Gene ontology enrichment analysis was done using Panther version 11.[83]

Inhibition of Kyneurinine-3-Monooxygenase

Mice were treated daily with Ro-61-8048 (Selleckchem, Houston, TX, USA; 10 mg/kg/day, oral) or vehicle (2% DMSO, 30% polyethylene glycol, 5% Tween, in water) for 3 days prior to blast injury, and continuously for the duration of the study. Mice exposed to blast to examine the role of KMO received one single 20-PSI injury. Control mice were exposed to sham injury.

Statistical Analysis

Results are expressed as mean ± SEM unless otherwise indicated. Analysis was conducted by experimenters blinded to the treatment condition of the sample or subject. Statistical comparisons were performed using GraphPad Prism (Ver. 4.0, GraphPad Software, San Diego, CA, USA).

RESULTS

Single and Multiple Blast Exposures Result in Similar Levels of RGC Damage and Dysfunction

We used PERG to investigate whether multiple blast exposures resulted in worse RGC functional outcomes compared to sham-exposed or mice with a single blast exposure 16 weeks after blast exposure. Sham blast mice had a PERG response amplitude of 27.42 ± 2.00 μV ($n = 16$). A decrease in the PERG amplitude was observed in mice receiving a single blast exposure (sTBI) ($n = 15$; sTBI, 13.85 ± 1.42 μV, $P = 0.0001$), three blast exposures with a 1-week interblast interval (wTBI) ($n = 16$; wTBI, 17.93 ± 2.45 μV, $P = 0.0040$), and three blast exposures with a 1-hour interval (hTBI) ($n = 13$; hTBI, 16.37 ± 2.18 μV, $P = 0.0014$, 1-way ANOVA with Dunnett's multiple comparison test) (Fig. 1), compared to sham blast mice. Unexpectedly, there was no difference when comparing the PERG amplitude of single blast sTBI mice to either the 1-week interval (wTBI, $P = 0.3596$) or 1-hour interval (hTBI, $P =$

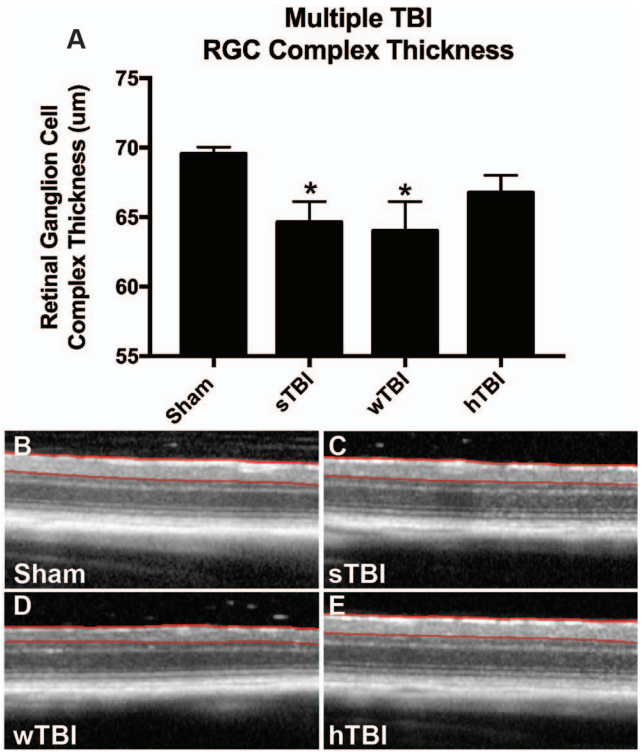

FIGURE 2. In order to determine if retinal function and structure followed a similar pattern of loss, we used optical coherence tomography to analyze the thickness of the RGC complex. The RGC complex thickness of sham blast mice was 69.56 ± 0.49 μm (**A**, **B**). We noted significant thinning of the RGC complex in sTBI-treated mice (**A**, **C**; 64.62 ± 1.51 μm, $P = 0.0377$) and wTBI-treated mice (**A**, **D**; 64.01 ± 2.11 μm, $P = 0.0220$), but not in hTBI-treated mice (**A**, **E**; 66.76 ± 1.25 μm, $P = 0.3626$, 1-way ANOVA with Dunnett's multiple comparison test). There was not a difference when comparing sTBI mice with either wTBI-treated mice ($P = 0.9817$), or hTBI-treated mice ($P = 0.5732$, 1-way ANOVA with Dunnett's multiple comparison test).

0.7430, 1-way ANOVA with Dunnett's multiple comparison test), repeatedly blasted groups of mice.

In order to determine if retinal function and structure followed a similar pattern of loss, we used optical coherence tomography (OCT) to analyze the thickness of the RGC complex layer. The RGC complex thickness of sham blast mice was 69.56 ± 0.49 μm. We noted significant thinning of the RGC complex in sTBI (64.62 ± 1.51 μm, $P = 0.0377$)- and wTBI (64.01 ± 2.11 μm, $P = 0.0220$)-treated mice, but not in hTBI-treated mice (66.76 ± 1.25 μm, $P = 0.3626$, 1-way ANOVA with Dunnett's multiple comparison test (Fig. 2) compared to sham blast mice. There was not a difference when comparing sTBI mice with either wTBI ($P = 0.9817$) or hTBI treated mice ($P = 0.5732$, 1-way ANOVA with Dunnett's multiple comparison test). Quantification of the outer nuclear layer (ONL) demonstrated there was no change in thickness when sham-blasted mice (56.39 ± 1.26 μm) were compared to sTBI (54.09 ± 2.62, $P = 0.7718$), wTBI (57.19 ± 0.91, $P = 0.9879$), or hTBI (56.79 ± 1.44, $P = 0.9983$; Supplementary Fig. S2A, 1-way ANOVA with Dunnett's multiple comparison test). No differences between sTBI, wTBI, or hTBI were observed ($P > 0.05$). Quantification of the total retinal thickness of sham mice was 165.8 ± 1.76 μm. A significant thinning was observed in sTBI mice (150.8 ± 5.51 μm, $P = 0.0207$, Supplementary Fig. S2B, 1-way ANOVA with Dunnett's multiple comparison test). There was not a significant difference between sham and wTBI (162.8 ± 2.65, $P = 0.9372$) or hTBI (161.0 ± 2.77 μm, $P = 0.7820$). There was no difference when comparing sTBI, wTBI, and hTBI ($P > 0.05$).

Unbiased immunohistochemical analysis was performed at the termination of the study to determine the density of BRN3A-positive RGCs present after sham blast exposure, single blast exposure, or multiple blast exposures (Fig. 3). Sham-treated mice had 2732 ± 78.56 RGCs/mm^2, which was greater than for the sTBI-treated mice (1987 ± 309.2 RGCs/mm^2, $P = 0.0268$). A trend toward decreased density was observed in wTBI-treated mice (2132 ± 159.1 RGCs/mm^2, $P = 0.0867$), and hTBI-treated mice (2339 ± 136.5 RGCs/mm^2, $P = 0.3460$, 1-way ANOVA with Dunnett's multiple comparison test), but did not reach statistical significance. There was no significant difference between sTBI and wTBI ($P = 0.9991$, 1-way ANOVA with Tukey's multiple comparison test) or between sTBI and hTBI ($P = 0.6588$).

Low-Intensity Blast Preconditioning Protects RGC Function and Structure

An unexpected result of our analysis of mice with multiple 20-PSI blast exposures separated by 1 week or 1 hour revealed that multiple exposures at these intervals did not result in more

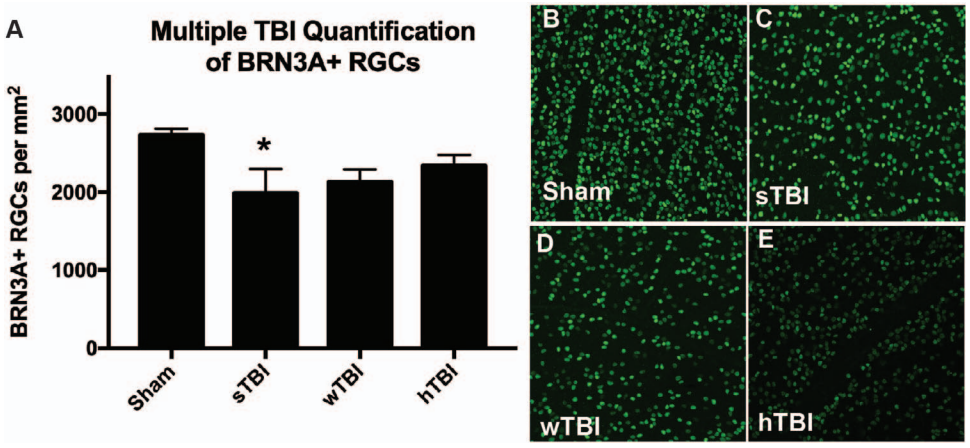

FIGURE 3. Multiple blast exposures do not cause greater RGC loss than single blast exposure. Histologic analysis of the number of BRN3A-positive (+) RGCs that remained after sham blast exposure, single blast exposure, or multiple blast exposures. Sham blast-treated mice had significantly more BRN3A+ RGCs than sTBI-treated mice (**A**–**C**; $P = 0.0268$), but not significantly more than wTBI (**A**, **D**; $P = 0.0867$) or hTBI mice (**E**; $P = 0.3460$ 1-way ANOVA with Dunnett's multiple comparison test).

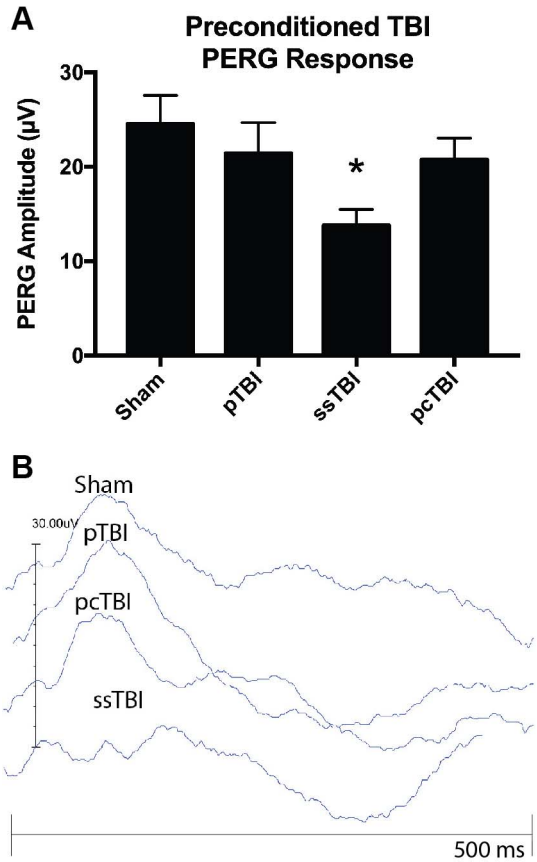

FIGURE 4. Low-level blast preconditioning protects RGC function. Mice preconditioned with a low-intensity blast and subsequently exposed to blast (pTBI, $n = 9$) or preconditioned control mice (pcTBI, $n = 9$) did not have significantly different PERG amplitudes compared to sham blast-exposed mice ($P = 0.7549$ and $P = 0.6084$, respectively). Mice receiving a single blast exposure (ssTBI, $n = 10$) of 137 kPa had significantly lower PERG amplitudes compared to sham blast (sham, $n = 9$)-exposed mice (**A**, **B**; $P = 0.0198$, 1-way ANOVA with Dunnett's multiple comparison test).

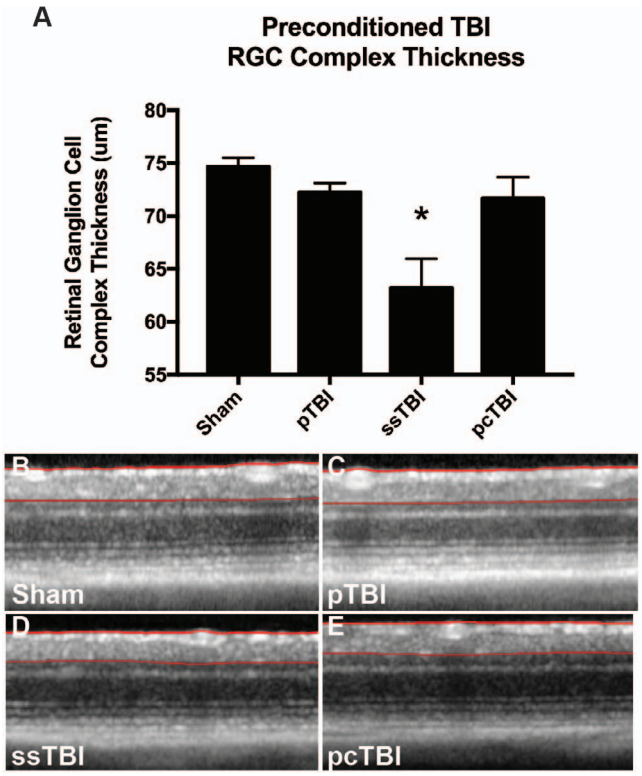

FIGURE 5. Blast preconditioning protects the structure of the RGC complex. Mice preconditioned with a low-intensity blast and subsequently exposed to blast (**A**, **C**; pTBI) or preconditioned control mice (**A**, **E**; pcTBI) did not have significantly different RGC complex thicknesses compared to sham blast-exposed mice (**A**, **B**; $P = 0.6004$ and $P = 0.4075$, respectively). Mice receiving a single blast injury (**A**, **D**; ssTBI) showed lower RGC complex thicknesses ($P = 0.0001$, 1-way ANOVA with Dunnett's multiple comparison test) when compared to sham.

damage to RGC function or structure than single blast exposures. In fact, structural analysis with OCT and histologic analysis of mice receiving multiple blast exposures separated by 1 hour did not show statistical differences from sham. This finding led us to hypothesize that initial blast exposures may activate endogenous pathways that offer acute neuroprotection to RGCs to repeat injury. In order to test this hypothesis, we examined mice exposed to different intensities of blast. Mice received a total of three injuries separated by 1 week. We examined sham blast mice (sham, sham, sham), preconditioned TBI mice (pTBI, 5 PSI, 5 PSI, 20 PSI), mice receiving a single injury (ssTBI, sham, sham, 20 PSI), and preconditioned control mice receiving three low-intensity blasts (pcTBI, 5 PSI, 5 PSI, 5 PSI).

We recorded the PERG to determine if preconditioning could protect RGC function (Fig. 4). PERG analysis revealed an amplitude of 24.53 ± 3.02 μV for sham blast mice ($n = 9$), which was not different compared to pTBI ($n = 9$, 21.42 ± 3.27 μV, $P = 0.7549$) or pcTBI mice ($n = 9$, 20.76 ± 2.27 μV, $P = 0.6084$). Mice receiving a single high-intensity blast exposure (ssTBI) had significantly lower PERG amplitudes ($n = 10$, 13.79 ± 1.70 μV, $P = 0.0198$, 1-way ANOVA with Dunnett's multiple comparison test) when compared to sham blast mice.

Structural analysis of the RGC complex thickness showed that sham blast mice (74.66 ± 0.85 μm) did not differ from pTBI (72.26 ± 0.84 μm, $P = 0.6004$) or pcTBI (71.65 ± 0.64 μm, $P = 0.4075$) mice (Fig. 5). Mice receiving a single high-intensity injury showed decreased RGC complex thicknesses (63.21 ± 2.73 μm, $P = 0.0001$, 1-way ANOVA with Dunnett's multiple comparison test) when compared to sham.

These differences in retinal ganglion anatomy were confirmed by quantification of BRN3A-positive RGCs at the termination of the experiment (Fig. 6). Sham blast mice had 3023 ± 135.6 RGCs/mm^2, which was not different than pTBI (2529 ± 134.7 = 4 RGCs/mm^2, $P = 0.4719$) or pcTBI (2756 ± 104.7 RGCs/mm^2, $P = 0.8401$) mice. The ssTBI mice had fewer BRN3A-positive RGCs (1683 ± 611.8 RGCs/mm^2, $P = 0.0118$, 1-way ANOVA with Dunnett's multiple comparison test) when compared to sham.

Blast Preconditioning Results in Gene Upregulation

To more fully understand the molecular mechanisms responsible for protection of RGCs after preconditioning, three groups of mice were analyzed: blasted mice ($n = 8$, 0 PSI, 20 PSI), preconditioned mice ($n = 8$, 5 PSI, 20 PSI), and preconditioned control mice ($n = 8$, 5 PSI, 5 PSI), with a 1-week interblast interval. Analysis of gene changes between blasted mice and sham blast mice revealed significant differences in the expression of 639 genes (Figs. 7A, 7B; Supplementary Table S1. Analysis of changes between blasted mice and preconditioned mice revealed 271 transcripts with significant changes in gene expression (Figs. 7A, 7C; Supple-

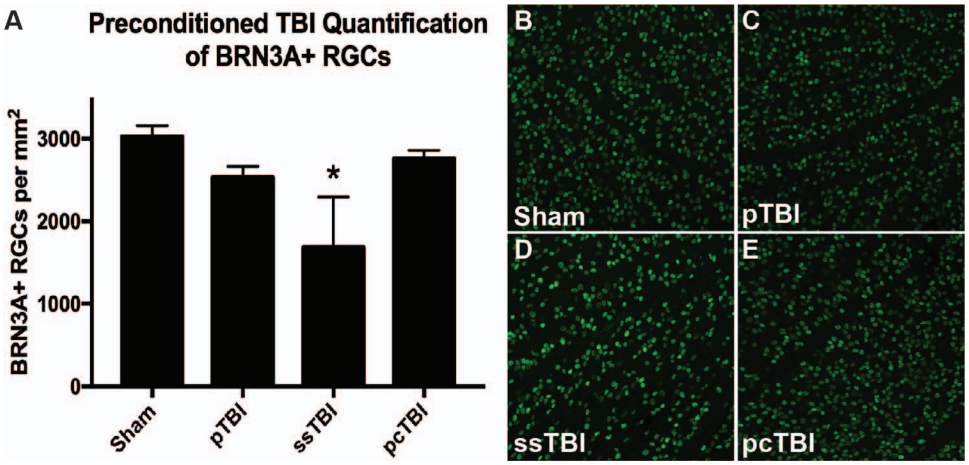

FIGURE 6. Low-level blast preconditioning results in RGC soma preservation. Mice exposed to a preconditioning blast (**A**, **C**; pTBI) or preconditioned control mice (**A**, **E**; pcTBI) did not have a significantly decreased number of surviving BRN3A+ RGCs compared to sham blast mice (**A**, **B**; $P = 0.4719$ and $P = 0.8401$, respectively), although there was a trend toward decreased cell survival. Mice exposed to one single injury had fewer BRN3A+ RGCs (**A**, **D**; $P = 0.0118$, 1-way ANOVA with Dunnett's multiple comparison test) when compared to sham.

mentary Table S2). Interestingly, only 7 of these transcripts were unique to this comparison, with the other 264 also different between sham and blast (Supplementary Table S3). Comparison of preconditioned control mice with preconditioned mice revealed no statistically significant transcriptomic changes (Fig. 7D; Supplementary Table S4). RNA-seq data are available for reanalysis and redisplay at the NCBI Gene Expression Omnibus (study identification GSE133940). The seven unique transcripts that were changed included *Cd40* (ENSMUSG00000017652), *Mrpl34* (ENSMUSG00000034880), *Kmo* (ENSMUSG00000039783), *Lmcd1* (ENSMUSG00000057604), *BC030870* (ENSMUSG00000074300), *I830077J02Rik* (ENSMUSG00000074342), and *Ms4a14* (ENSMUSG00000099398).

Targets Identified by RNA-seq Are Functionally Relevant

We sought to validate the biological relevance of a single transcript identified by RNA-seq through the process of inhibiting KMO with a noncompetitive inhibitor, previously shown to be effective in vivo. At 5 weeks after a single blast exposure the PERG amplitudes were 31.79 ± 2.48 (sham, $n = 8$), 19.87 ± 1.83 (blast + vehicle, $n = 8$), and 30.28 ± 4.04 (blast + Ro 61-8048, $n = 7$) (Fig. 8A). Blast + vehicle mice had lower PERG amplitudes than sham blast mice ($P = 0.0166$, 1-way ANOVA with Tukey's multiple comparison test) and blast + Ro 61-8048 mice ($P = 0.0456$). There was no difference in the PERG amplitudes when comparing sham blast mice and blast + Ro 61-8048–treated mice ($P = 0.9267$).

SD-OCT analyses of retinal thicknesses were 70.17± 0.45 µm (sham blast), 66.61±0.68 µm (blast + vehicle), and 69.91 ± 1.11 µm (blast + Ro 61-8048) (Fig. 8B). Blast vehicle-treated mice had decreased RGC complex thickness compared to sham blast mice ($P = 0.0085$, 1-way ANOVA with Tukey's multiple comparison test) and blast + Ro 61-8048 mice ($P = 0.0163$). There was no difference between sham blast mice and blast + Ro 61-8048 mice ($P = 0.9823$).

DISCUSSION

The purpose of this study was to determine if multiple blast exposures resulted in greater damage to RGCs than a single blast exposure. Here we show that both single and multiple blast exposures result in decreased RGC function compared to sham-treated mice; however, mice blasted more than once did not have worse outcomes than mice receiving a single injury. An unexpected finding was that preconditioning mice with a low-intensity blast protects RGCs from subsequent higher-intensity blasts. Transcriptional analysis of mice identified several genes as likely candidates that mediate these neuroprotective effects. Furthermore, we demonstrated that inhibition of one key enzyme uncovered during this study, KMO, could protect RGCs from blast-mediated structural and functional loss.

It is widely known that the visual system can be damaged by a TBI, with both acute and chronic dysfunction observed. Previous studies have demonstrated anatomic disruption of the inner retina, outer retina, and/or optic nerve. Light-evoked functional responses are affected by blast exposure, and deficits in gross visual function such as spatial frequency and contrast sensitivity[84] have been observed in both laboratory models and human subjects. Injuries due to a single blast or concussive exposure have been widely studied, with less emphasis placed on examining the effect of repeated injuries in the visual system. Some of the first studies of repetitive injury that focused on the visual system have suggested that these injuries are additive and cumulative.[32,33] Repetitive concussive injury via weight drop has been shown to result in demyelination of the optic nerve and loss of RGCs.[33] Likewise, repeated blast exposures have been shown to increase optic nerve damage compared to one single blast injury,[32] and greater anatomic damage.[34] In light of these previous reports, it is surprising that multiple blast exposures did not result in increased RGC loss compared to one single blast exposure. These findings may be open to several different explanations. It is possible that one single 20-PSI blast damages the visual system in such a way that no other subsequent equivalent injuries will result in increased damage. Although we examined these retinas 16 weeks following blast exposure, there is also the possibility that ongoing retinal degenerative processes would result in greater damage in the cohorts of mice receiving multiple injuries if they were allowed to age. There is a possibility that while the raw functional and structural responses were similar in magnitude, the molecular pathways eliciting those responses were vastly different among groups.

Due to the lack of difference between mice exposed to one or three blasts, we hypothesized that multiple blast exposure

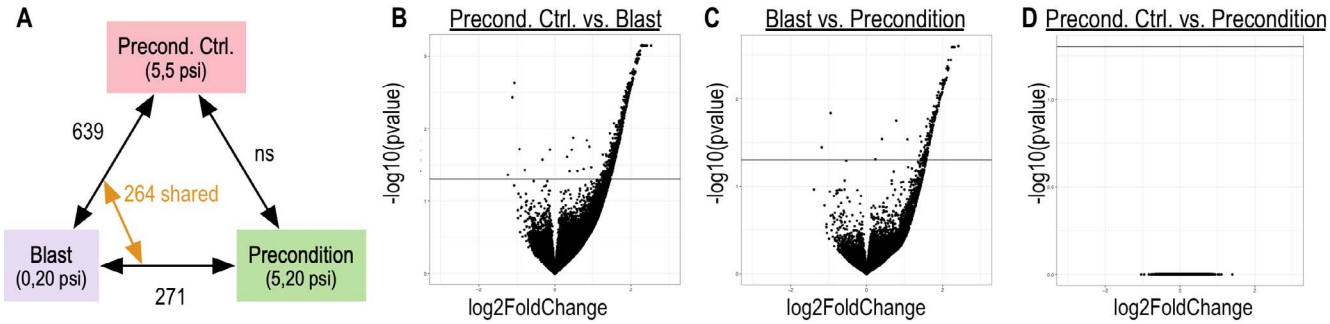

Figure 7. RNA-seq analysis reveals gene expression changes between blasted and preconditioned mice. Three groups of mice were analyzed: blasted mice (0 PSI, 20 PSI), preconditioned mice (5 PSI, 20 PSI), and preconditioned control (Precond. Ctrl. mice, 5 PSI, 5 PSI). Analysis of gene changes between blasted mice and preconditioned control mice revealed 639 statistically significant changes in genes (**A**, **B**), and 271 statistically significant changes in genes between blast-exposed mice and blast-preconditioned mice (**A**, **C**), with only 7 unique genes in this group. Analysis of transcript changes between preconditioned control mice and preconditioned mice revealed no significant changes (ns, **A**, **D**).

may upregulate protective factors and/or downregulate factors that lead to neuronal damage. In order to test this hypothesis, we compared mice that had been exposed to one single blast to mice that had been exposed to two low-level preconditioning blasts prior to a 20-PSI blast injury. Preconditioning has been widely studied related to stroke, ischemic events, and oxidative stress.[85,86] Overwhelmingly, these studies have demonstrated that preconditioning cells and tissues with brief, nonlethal events prior to a large stroke or infarct leads to improved outcomes. The evidence from these studies suggests that preconditioning events protect cells and tissue by upregulating endogenous survival factors, or downregulating factors that cause damage. In our study we used low-intensity blasts of 5 PSI prior to a 20-PSI injury, and showed protection of RGC structure and function in the preconditioned animals compared to animals receiving a single blast. It should be noted that there was a trend toward decreased responses in both the preconditioned blast mice and the preconditioned control mice receiving three 5-PSI injuries, but the decrease did not reach statistical significance. There is a possibility that while low-intensity injuries upregulate endogenous survival factors, they also induce some amount of damage.

In order to define some of the molecular pathways that shape the RGC response to blast injury in C57BL/6J mice, we performed RNA-seq analysis on preconditioned control mice, blast-exposed mice, and preconditioned blast mice. Comparison of blast mice and sham blast mice revealed 639 changed transcripts. Comparison of blast mice and preconditioned mice revealed 271 changes, with only 7 unique transcripts in this group. Most of these transcripts are associated with genes that are uncharacterized or lightly characterized. However, one gene, KMO, has been implicated in cell loss in neurologic disease and injury. KMO is a flavin adenine dinucleotide (FAD) dependent monoxygenase, which resides on the outer mitochondrial membrane. KMO is expressed in multiple cell types, including microglia, astrocytes, and mononuclear cells from the peripheral blood.[87] KMO is an enzyme functioning in the kynurenine pathway of tryptophan degradation that catalyzes the hydroxylation of L-kynurenine (L-KYN) to form the compound 3-hydroxy-L-kynurenine (3-HK), which is subsequently converted to quinolinic acid (QA), a neurotoxin and NMDA receptor antagonist. Both 3-HK and QA are linked to neurotoxic effects while the alternative product of the pathway, kynurenic acid (KYNA), is linked to neuroprotective

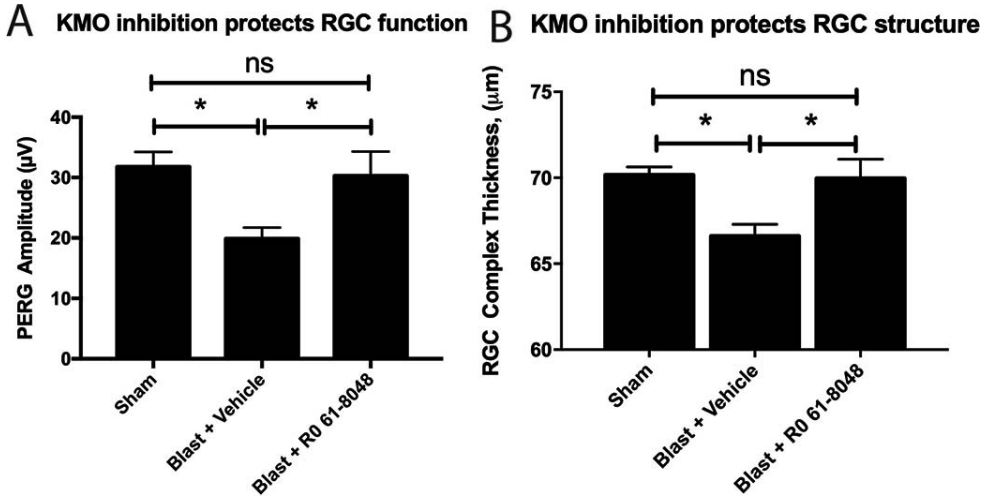

Figure 8. Inhibition of kyneurinine-3-monoxygenase results in preservation of RGC function and structure. Mice were treated daily with Ro-61-8048 for 3 days prior to blast injury, and continuously for the duration of the study. Five weeks after blast exposure, vehicle-treated blast-exposed mice (Blast + Vehicle) had significantly lower PERG responses than sham blast mice (Sham, $P = 0.0166$) or blast-exposed mice treated with Ro-61-8048 (**A**; Blast + Ro-61-8048, $P = 0.0456$, 1-way ANOVA with Tukey's multiple comparison test). There was no difference between sham blast mice and Ro-61-8048–treated mice ($P = 0.9267$). Analysis of the RGC complex thickness revealed a similar trend, with vehicle-treated blast mice having decreased RGC complex thickness compared to sham blast mice ($P = 0.0085$) and blast-exposed mice treated with Ro-61-8048 (**B**; $P = 0.0163$, 1-way ANOVA with Tukey's multiple comparison test). There was no difference between sham blast mice and Ro 61-8048 mice ($P = 0.9823$).

effects in the CNS.[87] The kynurenine pathway (KP) has been linked to inflammation, the immune system, and neurologic conditions including schizophrenia, Alzheimer's disease (AD), major depressive disorder (MDD), Parkinson's disease (PD), and Huntington's disease (HD).[88,89] An increase in QA has been reported in one study of humans with TBI.[90] Kynurenine is transported to the brain, and converted into KYNA by astrocytes, where KYNA aids in neuroprotection by decreasing glutamate levels. There may be other mechanisms of action surrounding the decrease of neuroinflammation linked to an increase in KYNA and inhibition of KMO.[91] Likewise, inhibition of KMO in peripheral monocytes results in improved outcomes in mouse models of AD.[91] Additionally, microglial cells are influential in KP metabolism. Microglia regulate the pathway by preferentially producing oxidative metabolites, including QA. In healthy individuals, kynurenine is metabolized to KYNA by astrocytes. However, in individuals with neurologic disease, increased concentrations of 3-HK and QA have been detected. It has also been noted that inhibition of KMO results in a decreased proinflammatory response from microglial cells.[92] We have shown here that inhibition of KMO with Ro-61-8048 results in preservation of RGC structure and function. Interestingly, Ro-61-8048 does not readily cross the blood brain–barrier, suggesting that most of the effect observed in our studies is mediated by inhibition of KMO in peripheral monocytes, which prevents a reciprocal upregulation in the retina. We hypothesize that the increased RGC spontaneous activity we have previously observed,[71] in addition to the increased responses observed after TBI in a recent study,[3] is partly due to an increase in QA, and its effect on NMDA receptors. The mechanism for KMO upregulation following blast injury is still unclear.

While this study has demonstrated several novel findings, there are some limitations of this study that should be noted, which may impact interpretation of our results. First, we did not perform full-field ERGs so we cannot discount the possibility of outer retinal functional deficits influencing the reduction in PERG amplitude observed in our studies. Additionally, while the OCT analysis revealed a normal outer nuclear layer and overall retinal structure, we did not perform rigorous histologic analysis for other retinal layers. There is a potential that edema or dendritic reorganization in the RGC complex is artificially increasing the thickness in some groups, which is an important topic we intend to investigate in future studies. While we have shown that blast preconditioning protects RGCs compared to mice exposed to one single 20-PSI injury, we do not yet understand the duration of the effect. For example, there is a possibility that blast preconditioning inhibits only mechanisms that cause acute RGC damage, but do not affect long-term RGC survival. There is a potential that if blast-preconditioned mice were aged to 16 weeks following injury they would show the same levels of RGC degeneration as mice exposed to a single or multiple blasts at that age. Since this is a possibility, the results shown here need to be interpreted as showing that blast preconditioning can prevent structural and functional RGC decreases up to 8 weeks following injury.

For our RNA-seq studies we intentionally evaluated transcriptional changes acutely following blast exposure to examine changes and identify genes that potentially mediate neuroprotection. There is a potential that the changes we identified are secondary to other transcriptional changes occurring in the retina. While this is possible, at least one change that we have identified, KMO, was validated as functionally relevant to blast-mediated TBI pathology. Furthermore, the transcriptional changes that we have identified were from all cell classes in the retina, and only from RGCs. Due to the small percentage of RGCs compared to all other cells in the retina, it is possible that genes with high relevance to RGC loss have not been identified in this study due to the low expression of the transcripts. Future studies will focus on collecting samples more densely after injury, in addition to assessing individual cell classes, particularly RGCs.

In conclusion, we have demonstrated that blast preconditioning results in neuroprotection of RGCs that is mediated, at least in part, by KMO. While we are not suggesting that preconditioning can be translated to humans with acquired TBI, it is worth noting that preconditioning may be a method to increase the resolution of gene analysis experiments to find functionally relevant genes and gene pathways. Also, inhibition of specific enzymes and pathways may lead to other targets following acquired TBI. There is potential for development of KMO inhibitors or modulators to increase recovery following TBI, or to prevent chronic neuronal damage. This transcriptomic study was conducted in only one strain of inbred mice, and within a defined window of time after blast injury. It is possible that discovery of more complex gene networks that shape the neuronal response to blast injury is possible by using different inbred or outbred lines of mice, varying the blast exposure intensity, and examining the responses at different time points after blast.

Acknowledgments

The authors thank Carly J. van der Heide for providing the protocol to quantify BRN3A-positive cells.

Supported by the Department of Veterans Affairs (RX000952); the Department of Defense (W81XWH-14-1-0583); the Iowa City VA Center for the Prevention and Treatment of Visual Loss; Career Development/Capacity Building Award IK2-RX002003 from the U.S. Department of Veterans Affairs Rehabilitation Research and Development (Rehab. R&D) Service (LMD); Training Grant T32 DK112751-01 (AH-B). The RNA-seq were obtained at the Genomics Division of the Iowa Institute of Human Genetics, which is supported, in part, by the University of Iowa Carver College of Medicine. The authors alone are responsible for the content and writing of the paper.

Disclosure: **M.M. Harper**, None; **A.W. Woll**, None; **L.P. Evans**, None; **M. Delcau**, None; **A. Akurathi**, None; **A. Hedberg-Buenz**, None; **D.A. Soukup**, None; **N. Boehme**, None; **M.M. Hefti**, None; **L.M. Dutca**, None; **M.G. Anderson**, None; **A.G. Bassuk**, None

References

1. Sawyer TW, Wang Y, Ritzel DV, et al. High-fidelity simulation of primary blast: direct effects on the head. *J Neurotrauma*. 2016;33:1181–1193.
2. Goldstein LE, Fisher AM, Tagge CA, et al. Chronic traumatic encephalopathy in blast-exposed military veterans and a blast neurotrauma mouse model. *Sci Transl Med*. 2012;4:134ra60.
3. Allen RS, Motz CT, Feola A, et al. Long-term functional and structural consequences of primary blast overpressure to the eye. *J Neurotrauma*. 2018;35:2104–2116.
4. Cernak I, Wang Z, Jiang J, Bian X, Savic J. Ultrastructural and functional characteristics of blast injury-induced neurotrauma. *J Trauma*. 2001;50:695–706.
5. Cho RI, Bakken HE, Reynolds ME, Schlifka BA, Powers DB. Concomitant cranial and ocular combat injuries during Operation Iraqi Freedom. *J Trauma*. 2009;67:516–520, discussion 519–520.
6. Guley NH, Rogers JT, Del Mar NA, et al. A novel closed-head model of mild traumatic brain injury using focal primary overpressure blast to the cranium in mice. *J Neurotrauma*. 2016;33:403–422.

7. Hines-Beard J, Marchetta J, Gordon S, Chaum E, Geisert EE, Rex TS. A mouse model of ocular blast injury that induces closed globe anterior and posterior pole damage. *Exp Eye Res*. 2012;99:63–70.
8. Huber BR, Meabon JS, Martin TJ, et al. Blast exposure causes early and persistent aberrant phospho- and cleaved-tau expression in a murine model of mild blast-induced traumatic brain injury. *J Alzheimers Dis*. 2013;37:309–323.
9. Kuehn R, Simard PF, Driscoll I, et al. Rodent model of direct cranial blast injury. *J Neurotrauma*. 2011;28:2155–2169.
10. Lemke S, Cockerham GC, Glynn-Milley C, Lin R, Cockerham KP. Automated perimetry and visual dysfunction in blast-related traumatic brain injury. *Ophthalmology*. 2016;123:415–424.
11. Song H, Cui J, Simonyi A, et al. Linking blast physics to biological outcomes in mild traumatic brain injury: narrative review and preliminary report of an open-field blast model. *Behav Brain Res*. 2018;340:147–158.
12. Song H, Konan LM, Cui J, et al. Ultrastructural brain abnormalities and associated behavioral changes in mice after low-intensity blast exposure. *Behav Brain Res*. 2018;347:148–157.
13. Swan AA, Nelson JT, Pogoda TK, Amuan ME, Akin FW, Pugh MJ. Sensory dysfunction and traumatic brain injury severity among deployed post-9/11 veterans: a Chronic Effects of Neurotrauma Consortium study. *Brain Inj*. 2018;32:1197–1207.
14. Zander NE, Piehler T, Boggs ME, Banton R, Benjamin R. In vitro studies of primary explosive blast loading on neurons. *J Neurosci Res*. 2015;3:1353–1363.
15. Gallun FJ, Diedesch AC, Kubli LR, et al. Performance on tests of central auditory processing by individuals exposed to high-intensity blasts. *J Rehabil Res Dev*. 2012;49:1005–1025.
16. Gallun FJ, Lewis MS, Folmer RL, et al. Implications of blast exposure for central auditory function: a review. *J Rehabil Res Dev*. 2012;49:1059–1074.
17. Saunders GH, Frederick MT, Arnold M, Silverman S, Chisolm TH, Myers P. Auditory difficulties in blast-exposed veterans with clinically normal hearing. *J Rehabil Res Dev*. 2015;52:343–360.
18. Couch JR, Stewart KE. Headache prevalence at 4-11 years after deployment-related traumatic brain injury in veterans of Iraq and Afghanistan wars and comparison to controls: a matched case-controlled study. *Headache*. 2016;56:1004–1021.
19. Ryan-Gonzalez C, Kimbrel NA, Meyer EC, et al. Differences in post-traumatic stress disorder symptoms among post-9/11 veterans with blast- and non-blast mild traumatic brain injury. *J Neurotrauma*. 2019;36:1584–1590.
20. Sullivan DR, Hayes JP, Lafleche G, Salat DH, Verfaellie M. Functional brain alterations associated with cognitive control in blast-related mild traumatic brain injury. *J Int Neuropsychol Soc*. 2018;24:662–672.
21. Bjork JM, Burroughs TK, Franke LM, et al. Laboratory impulsivity and depression in blast-exposed military personnel with post-concussion syndrome. *Psychiatry Res*. 2016;246:321–325.
22. Capo-Aponte JE, Jorgensen-Wagers KL, Sosa JA, et al. Visual dysfunctions at different stages after blast and non-blast mild traumatic brain injury. *Optom Vis Sci*. 2017;94:7–15.
23. Needham CE, Ritzel D, Rule GT, Wiri S, Young L. Blast testing issues and TBI: experimental models that lead to wrong conclusions. *Front Neurol*. 2015;6:72.
24. Meabon JS, Huber BR, Cross DJ, et al. Repetitive blast exposure in mice and combat veterans causes persistent cerebellar dysfunction. *Sci Transl Med*. 2016;8:321ra6.
25. Peskind ER, Petrie EC, Cross DJ, et al. Cerebrocerebellar hypometabolism associated with repetitive blast exposure mild traumatic brain injury in 12 Iraq war veterans with persistent post-concussive symptoms. *Neuroimage*. 2011;54(suppl 1):S76–S82.
26. Petrie EC, Cross DJ, Yarnykh VL, et al. Neuroimaging, behavioral, and psychological sequelae of repetitive combined blast/impact mild traumatic brain injury in Iraq and Afghanistan war veterans. *J Neurotrauma*. 2014;31:425–436.
27. Walker WC, Franke LM, Sima AP, Cifu DX. Symptom trajectories after military blast exposure and the influence of mild traumatic brain injury. *J Head Trauma Rehabil*. 2017;32:E16–E26.
28. Carr W, Polejaeva E, Grome A, et al. Relation of repeated low-level blast exposure with symptomology similar to concussion. *J Head Trauma Rehabil*. 2015;30:47–55.
29. Carr W, Stone JR, Walilko T, et al. Repeated low-level blast exposure: a descriptive human subjects study. *Mil Med*. 2016;181(5 suppl):28–39.
30. Rhea CK, Kuznetsov NA, Ross SE, et al. Development of a portable tool for screening neuromotor sequelae from repetitive low-level blast exposure. *Mil Med*. 2017;182:147–154.
31. Tate CM, Wang KK, Eonta S, et al. Serum brain biomarker level, neurocognitive performance, and self-reported symptom changes in soldiers repeatedly exposed to low-level blast: a breacher pilot study. *J Neurotrauma*. 2013;30:1620–1630.
32. Vest V, Bernardo-Colón A, Watkins D, Kim B, Rex TS. Rapid repeat exposure to subthreshold trauma causes synergistic axonal damage and functional deficits in the visual pathway in a mouse model. *J Neurotrauma*. 2019;36:1646–1654.
33. Tzekov R, Dawson C, Orlando M, et al. Sub-chronic neuropathological and biochemical changes in mouse visual system after repetitive mild traumatic brain injury. *PLoS One*. 2016;11:e0153608.
34. Choi JH, Greene WA, Johnson AJ, et al. Pathophysiology of blast-induced ocular trauma in rats after repeated exposure to low-level blast overpressure. *Clin Exp Ophthalmol*. 2015;43:239–246.
35. Fehily B, Fitzgerald M. Repeated mild traumatic brain injury: potential mechanisms of damage. *Cell Transplant*. 2017;26:1131–1155.
36. Weil ZM, Gaier KR, Karelina K. Injury timing alters metabolic, inflammatory and functional outcomes following repeated mild traumatic brain injury. *Neurobiol Dis*. 2014;70:108–116.
37. Bolton AN, Saatman KE. Regional neurodegeneration and gliosis are amplified by mild traumatic brain injury repeated at 24-hour intervals. *J Neuropathol Exp Neurol*. 2014;73:933–947.
38. Mouzon B, Chaytow H, Crynen G, et al. Repetitive mild traumatic brain injury in a mouse model produces learning and memory deficits accompanied by histological changes. *J Neurotrauma*. 2012;29:2761–2773.
39. Hylin MJ, Orsi SA, Rozas NS, et al. Repeated mild closed head injury impairs short-term visuospatial memory and complex learning. *J Neurotrauma*. 2013;30:716–726.
40. Kane MJ, Angoa-Pérez M, Briggs DI, Viano DC, Kreipke CW, Kuhn DM. A mouse model of human repetitive mild traumatic brain injury. *J Neurosci Methods*. 2012;203:41–49.
41. Shitaka Y, Tran HT, Bennett RE, et al. Repetitive closed-skull traumatic brain injury in mice causes persistent multifocal axonal injury and microglial reactivity. *J Neuropathol Exp Neurol*. 2011;70:551–567.
42. Laurer HL, Bareyre FM, Lee VM, et al. Mild head injury increasing the brain's vulnerability to a second concussive impact. *J Neurosurg*. 2001;95:859–870.
43. Fujita M, Wei EP, Povlishock JT. Intensity- and interval-specific repetitive traumatic brain injury can evoke both axonal and microvascular damage. *J Neurotrauma*. 2012;29:2172–2180.

Investigative Ophthalmology & Visual Science

44. Luo J, Nguyen A, Villeda S, et al. Long-term cognitive impairments and pathological alterations in a mouse model of repetitive mild traumatic brain injury. *Front Neurol*. 2014; 5:12.
45. Longhi L, Saatman KE, Fujimoto S, et al. Temporal window of vulnerability to repetitive experimental concussive brain injury. *Neurosurgery*. 2005;56:364–374, discussion 364–374.
46. Bennett RE, Mac Donald CL, Brody DL. Diffusion tensor imaging detects axonal injury in a mouse model of repetitive closed-skull traumatic brain injury. *Neurosci Lett*. 2012;513: 160–165.
47. Namjoshi DR, Cheng WH, McInnes KA, et al. Merging pathology with biomechanics using CHIMERA (Closed-Head Impact Model of Engineered Rotational Acceleration): a novel, surgery-free model of traumatic brain injury. *Mol Neurodegener*. 2014;9:55.
48. Bolton Hall AN, Joseph B, Brelsfoard JM, Saatman KE. Repeated closed head injury in mice results in sustained motor and memory deficits and chronic cellular changes. *PLoS One*. 2016;11:e0159442.
49. DeFord SM, Wilson MS, Rice AC, et al. Repeated mild brain injuries result in cognitive impairment in B6C3F1 mice. *J Neurotrauma*. 2002;19:427–438.
50. Meehan WP III, Zhang J, Mannix R, Whalen MJ. Increasing recovery time between injuries improves cognitive outcome after repetitive mild concussive brain injuries in mice. *Neurosurgery*. 2012;71:885–891.
51. Kawoos U, Abutarboush R, Zarriello S, et al. N-acetylcysteine amide ameliorates blast-induced changes in blood-brain barrier integrity in rats. *Front Neurol*. 2019;10:650.
52. Bugay V, Bozdemir E, Vigil FA, et al. A mouse model of repetitive blast traumatic brain injury reveals post-trauma seizures and increased neuronal excitability [published online ahead of print April 26, 2019]. *J Neurotrauma*. doi:10.1089/neu.2018.6333.
53. Badea A, Kamnaksh A, Anderson RJ, Calabrese E, Long JB, Agoston DV. Repeated mild blast exposure in young adult rats results in dynamic and persistent microstructural changes in the brain. *Neuroimage Clin*. 2018;18:60–73.
54. Calabrese E, Du F, Garman RH, et al. Diffusion tensor imaging reveals white matter injury in a rat model of repetitive blast-induced traumatic brain injury. *J Neurotrauma*. 2014;31: 938–950.
55. Prins ML, Alexander D, Giza CC, Hovda DA. Repeated mild traumatic brain injury: mechanisms of cerebral vulnerability. *J Neurotrauma*. 2013;30:30–38.
56. Arun P, Rittase WB, Wilder DM, Wang Y, Gist ID, Long JB. Defective methionine metabolism in the brain after repeated blast exposures might contribute to increased oxidative stress. *Neurochem Int*. 2018;112:234–238.
57. Arun P, Abu-Taleb R, Oguntayo S, et al. Acute mitochondrial dysfunction after blast exposure: potential role of mitochondrial glutamate oxaloacetate transaminase. *J Neurotrauma*. 2013;30:1645–1651.
58. Effgen GB, Ong T, Nammalwar S, et al. Primary blast exposure increases hippocampal vulnerability to subsequent exposure: reducing long-term potentiation. *J Neurotrauma*. 2016;33: 1901–1912.
59. DeKosky ST, Ikonomovic MD, Gandy S. Traumatic brain injury—football, warfare, and long-term effects. *N Engl J Med*. 2010;363:1293–1296.
60. Ikonomovic MD, Mi Z, Abrahamson EE. Disordered APP metabolism and neurovasculature in trauma and aging: combined risks for chronic neurodegenerative disorders. *Ageing Res Rev*. 2017;34:51–63.
61. Ikonomovic MD, Uryu K, Abrahamson EE, et al. Alzheimer's pathology in human temporal cortex surgically excised after severe brain injury. *Exp Neurol*. 2004;190:192–203.
62. Bandak FA, Long G, Bandak A, De Lanerolle NC, et al. Injury biomechanics, neuropathology, and simplified physics of explosive blast and impact mild traumatic brain injury. *Handb Clin Neurol*. 2015;127:89–104.
63. Zander NE, Piehler T, Hogberg H, Pamies D. Explosive blast loading on human 3D aggregate minibrains. *Cell Mol Neurobiol*. 2017;37:1331–1334.
64. Zander NE, Piehler T, Banton R, Boggs M. The effect of explosive blast loading on human neuroblastoma cells. *Anal Biochem*. 2016;504:4–6.
65. Eftaxiopoulou T, Barnett-Vanes A, Arora H, et al. Prolonged but not short-duration blast waves elicit acute inflammation in a rodent model of primary blast limb trauma. *Injury*. 2016;47: 625–632.
66. Laksari K, Sadeghipour K, Darvish K. Mechanical response of brain tissue under blast loading. *J Mech Behav Biomed Mater*. 2014;32:132–144.
67. Watson R, Gray W, Sponsel WE, et al. Simulations of porcine eye exposure to primary blast insult. *Trans Vis Sci Tech*. 2015;4(4):8.
68. Townsend MT, Alay E, Skotak M, Chandra N. Effect of tissue material properties in blast loading: coupled experimentation and finite element simulation [published online ahead of print December 6, 2018]. *Ann Biomed Eng*. doi:10.1007/s10439-018-02178-w.
69. Notghi B, Bhardwaj R, Bailoor S, et al. Biomechanical evaluations of ocular injury risk for blast loading. *J Biomech Eng*. 2017;139:081010.
70. Bailoor S, Bhardwaj R, Nguyen TD. Effectiveness of eye armor during blast loading. *Biomech Model Mechanobiol*. 2015;14: 1227–1237.
71. Dutca LM, Stasheff SF, Hedberg-Buenz A, et al. Early detection of subclinical visual damage after blast-mediated TBI enables prevention of chronic visual deficit by treatment with P7C3-S243. *Invest Ophthalmol Vis Sci*. 2014;55:8330–8341.
72. Mohan K, Kecova H, Hernandez-Merino E, Kardon RH, Harper MM. Retinal ganglion cell damage in an experimental rodent model of blast-mediated traumatic brain injury. *Invest Ophthalmol Vis Sci*. 2013;54:3440–3450.
73. Chou TH, Bohorquez J, Toft-Nielsen J, Ozdamar O, Porciatti V. Robust mouse pattern electroretinograms derived simultaneously from each eye using a common snout electrode. *Invest Ophthalmol Vis Sci*. 2014;55:2469–2475.
74. Mohan K, Kecova H, Hernandez-Merino E, Kardon RH, Harper MM. Retinal ganglion cell damage in an experimental rodent model of blast-mediated traumatic brain injury. *Invest Ophthalmol Vis Sci*. 2013;54:3440–3450.
75. Mohan K, Harper MM, Kecova H, et al. Characterization of structure and function of the mouse retina using pattern electroretinography, pupil light reflex, and optical coherence tomography. *Vet Ophthalmol*. 2012;15(suppl 2):94–104.
76. Hedberg-Buenz A, Christopher MA, Lewis CJ, et al. RetFM-J, an ImageJ-based module for automated counting and quantifying features of nuclei in retinal whole-mounts. *Exp Eye Res*. 2016; 146:386–392.
77. Baruzzo G, Hayer KE, Kim EJ, Di Camillo B, FitzHerald GA, Grant GR. Simulation-based comprehensive benchmarking of RNA-seq aligners. *Nat Methods*. 2017;14:135–139.
78. Dobin A, Davis CA, Schlesinger F, et al. STAR: ultrafast universal RNA-seq aligner. *Bioinformatics*. 2013;29:15–21.
79. Liao Y, Smyth GK, Shi W. featureCounts: an efficient general purpose program for assigning sequence reads to genomic features. *Bioinformatics*. 2014;30:923–930.
80. Anders S, Huber W. Differential expression analysis for sequence count data. *Genome Biol*. 2010;11:R106.
81. Hoffman GE, Schadt EE. variancePartition: interpreting drivers of variation in complex gene expression studies. *BMC Bioinformatics*. 2016;17:483.

Investigative Ophthalmology & Visual Science

82. Wickham H. *ggplot2: Elegant Graphics for Data Analysis*. New York: Springer Verlag; 2009.
83. Mi H, Huang X, Muruganujan A, et al. PANTHER version 11: expanded annotation data from Gene Ontology and Reactome pathways, and data analysis tool enhancements. *Nucleic Acids Res*. 2017;45:D183–D189.
84. Shedd DF, Benko NA, Jones J, Zaugg BE, Peiffer RL, Coats B. Long term temporal changes in structure and function of rat visual system after blast exposure. *Invest Ophthalmol Vis Sci*. 2018;59:349–361.
85. Basalay MV, Davidson SM, Gourine AV, Yellon DM. Neural mechanisms in remote ischaemic conditioning in the heart and brain: mechanistic and translational aspects. *Basic Res Cardiol*. 2018;113:25.
86. Chen G, Thakkar M, Robinson C, Doré S. Limb remote ischemic conditioning: mechanisms, anesthetics, and the potential for expanding therapeutic options. *Front Neurol*. 2018;9:40.
87. Abdel-Magid AF. Kynurenine monooxygenase (KMO) inhibitors for the treatment of acute pancreatitis and neurodegenerative disorders. *ACS Med Chem Lett*. 2015;6:954–955.
88. Davis I, Liu A. What is the tryptophan kynurenine pathway and why is it important to neurotherapeutics? *Expert Rev Neurother*. 2015;15:719–721.
89. Wonodi I, Stine OC, Sathyasaikumar KV, et al. Downregulated kynurenine 3-monooxygenase gene expression and enzyme activity in schizophrenia and genetic association with schizophrenia endophenotypes. *Arch Gen Psychiatry*. 2011; 68:665–674.
90. Yan EB, Frugier T, Lim CK, et al. Activation of the kynurenine pathway and increased production of the excitotoxin quinolinic acid following traumatic brain injury in humans. *J Neuroinflammation*. 2015;12:110.
91. Zwilling D, Huang SY, Sathyasaikumar KV, et al. Kynurenine 3-monooxygenase inhibition in blood ameliorates neurodegeneration. *Cell*. 2011;145:863–874.
92. Garrison AM, Parrott JM, Tuñon A, Delgado J, Redus L, O'Connor JC. Kynurenine pathway metabolic balance influences microglia activity: targeting kynurenine monooxygenase to dampen neuroinflammation. *Psychoneuroendocrinology*. 2018;94:1–10.

Investigative Ophthalmology & Visual Science